NANO LETTERS

Letter

pubs.acs.org/NanoLett

Ultrafast Electron Emission from a Sharp Metal Nanotaper Driven by Adiabatic Nanofocusing of Surface Plasmons

Jan Vogelsang,[†,‡] Jörg Robin,[†,‡] Benedek J. Nagy,[§,∥] Péter Dombi,[§] Daniel Rosenkranz,[†] Manuela Schiek,[†] Petra Groß,*[,†,‡] and Christoph Lienau*[,†,‡]

[†]Institut für Physik, Carl von Ossietzky Universität, 26129 Oldenburg, Germany

[‡]Center of Interface Science, Carl von Ossietzky Universität, 26129 Oldenburg, Germany

[§]Wigner Research Centre for Physics, 1121 Budapest, Hungary

[∥]Institute of Physics, University of Pécs, 7622 Pécs, Hungary

Supporting Information

ABSTRACT: We report photoelectron emission from the apex of a sharp gold nanotaper illuminated via grating coupling at a distance of 50 μm from the emission site with few-cycle near-infrared laser pulses. We find a fifty-fold increase in electron yield over that for direct apex illumination. Spatial localization of the electron emission to a nanometer-sized region is demonstrated by point-projection microscopic imaging of a silver nanowire. Our results reveal negligible plasmon-induced electron emission from the taper shaft and thus efficient nanofocusing of few-cycle plasmon wavepackets. This novel, remotely driven emission scheme offers a particularly compact source of ultrashort electron pulses of immediate interest for miniaturized electron microscopy and diffraction schemes with ultrahigh time resolution.

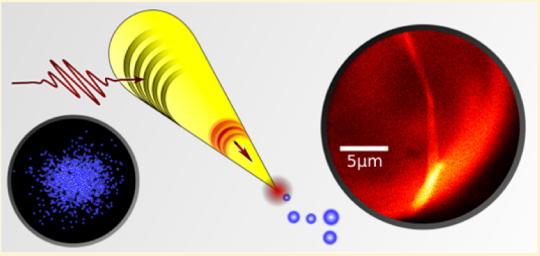

KEYWORDS: *ultrafast electron microscopy, adiabatic nanofocusing, surface plasmon polaritons, few-cycle light pulses, point projection electron microscopy, nanotip electron source*

Transmission electron microscopy offers, in modern, aberration-corrected microscopes, exquisite sub-Å spatial resolution and, thus, the most direct imaging of the atomic structure of matter.[1] Ideally, one would dream of combining such microscopes with a temporal resolution that is sufficient to directly visualize the motion of electrons and nuclei on their natural, atto- to femtosecond time scales, as reached in modern ultrafast laser spectroscopy. Consequently, research on ultrafast, laser-based electron microscopy started already in the 1980s, when Mourou and Williamson performed the first photoelectron-based diffraction experiments probing light-driven phase transitions with 20 ps time resolution.[2−4] In the 1990s, Zewail began his ground-breaking research on ultrafast electron microscopy, advancing the time resolution to <1 ps by incorporating a single-electron photocathode, driven by high-repetition rate lasers, into a high-spatial-resolution transmission electron microscope.[5,6] This time resolution has been improved to about 300 fs in a miniaturized diffraction setup, allowing visualization of, for example, nonthermal melting of aluminum.[7] In principle, it would be highly desirable to further enhance this temporal resolution because a variety of fundamental processes such as transiently induced superconductivity at elevated temperatures,[8] light-induced phase changes in strongly correlated materials,[9,10] or light-to-current conversion in organic solar cells[11] apparently invoke the correlated, coherent motion of electrons and nuclei on even faster time scales. This currently triggers much experimental activity in ultrafast electron imaging. Specifically, radiofrequency (RF) waves or potentially also terahertz waves may be used for temporal compression of electron pulses.[12−16] So far, this has led to the demonstration of electron bunch compression to less than 100 fs rms.[14] Further improvement in time resolution, possibly even below 10 fs,[17] may be expected when reducing space charge broadening and RF timing jitter.

An alternative imaging scheme, which has received renewed interest during the last years is point projection microscopy (PPM). With optimized field emitters, spatial resolution of a few nm is now readily achieved.[18−20] Recent activities[21−23] have combined such point projection microscopes with laser-triggered metal nanotaper emitters and, in first experiments, time-resolved imaging of photocurrents in InP-nanowires with ∼100 fs resolution has been demonstrated.[23] Several designs for compact electron sources are currently investigated in attempts to further improve temporal resolution and enhance measurement sensitivity. Ultimate temporal and spatial resolution in PPM requires minimization of the emitter-sample distance.[21] For currently used, laser-illuminated taper sources,[24,25] this is inevitably limited by the diffraction-limited focal spot size of the intense excitation laser. Reducing taper−sample distance below 10 μm, as appears to be necessary for bringing the time

Received: April 19, 2015
Revised: June 6, 2015
Published: June 10, 2015

DOI: 10.1021/acs.nanolett.5b01513
Nano Lett. 2015, 15, 4685−4691

resolution to less than 10 fs,[21] necessarily results in simultaneous sample illumination and, thus, in undesired sample heating or photoemission.[21]

Plasmonics may offer an elegant solution for this problem by avoiding direct far-field illumination of the taper apex. When launching ultrashort plasmon wavepackets on the shaft of a conical metallic nanotaper, the wavepacket spatially contracts as it approaches the apex, where it is focused into a nanometric volume well below the diffraction limit, resulting in a pronounced enhancement of the electric field at the very apex of the taper.[26−28] When using ultrashort light pulses for excitation, this enhanced field can become so large that nonlinear optical effects are induced. In all-optical studies of this adiabatic nanofocusing, grating coupling at distances of several tens of micrometers from the apex has been used to launch plasmon wavepackets.[29,30] A nanofocus spot size of 10 nm has been reached for plasmon pulses as short as 10 fs.[31,32] Such adiabatic compression of surface plasmons has recently been used, for example, for hot electron injection in a Schottky diode.[33]

Here, we employ this adiabatic nanofocusing concept for the first time to induce laser-driven field emission of electrons from the apex of a sharp gold taper, replacing far-field apex illumination by remotely driven plasmon nanofocusing. We realize a novel, compact source of ultrashort electron pulses of immediate interest for electron microscopy with ultimate time resolution. The properties of this electron source are rather intriguing. Even though plasmons propagate over mesoscopic distances along the taper shaft, electron emission stems solely from a nm-sized region at the very apex, as evidenced by PPM.

The central concept of our work is schematically illustrated in Figure 1a. Basically, we aim at replacing far-field optical excitation of laser-driven nanotip electron emitters,[24,34] which has recently become so important for exploring new regimes of strong-field physics[35,36] and coherent control of electron motion[35,37] and as sources for ultrafast electron microscopy or diffraction[23,38] by spatially localized, evanescent wave excitation. This shall provide us with a highly compact source of ultrafast low-energy pulses which can easily be integrated into miniaturized microscopy or diffraction setups.

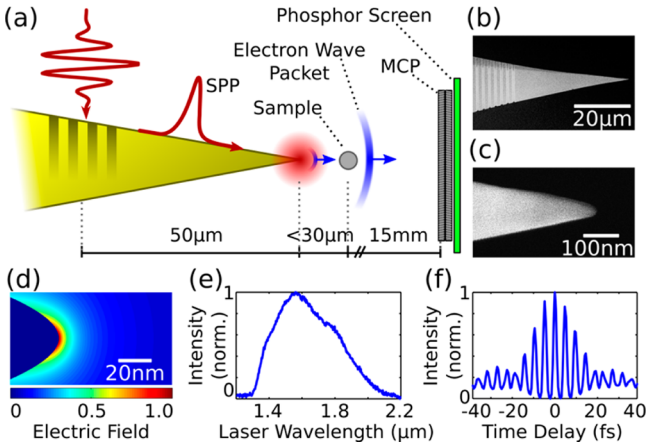

Figure 1. (a) Schematic of the setup for remotely driven electron emission. Few-cycle near-infrared light pulses are grating-coupled to a chemically etched gold taper. The launched SPP wavepacket propagates along the taper shaft and is nanofocused at the apex. The resulting strong field concentration leads to plasmon-induced electron emission. Electrons are detected in a point-projection setup using a microchannel plate equipped with a phosphor screen. (b) Scanning electron microscope image of a chemically etched gold taper. The grating coupler is fabricated by ion-beam milling. (c) Zoom of the apex region with a radius of curvature of 12 nm. (d) Simulated electric near-field distribution with a decay length of 8 nm. (e) Intensity spectrum and (f) interferometric autocorrelation function of the 16 fs near-infrared laser pulses.

For this, we make use of surface plasmon polariton (SPP) propagation and adiabatic nanofocusing of SPP wavepackets on conical metallic tapers. For such tapers, the negative real part of the dielectric function of the metal core ensures that the evanescent decay length of a bound SPP wave on the air side of the taper decreases continuously with decreasing taper radius as soon as the wire diameter is below one optical wavelength.[27,29] Thus, the effective refractive index of the bound SPP mode gradually increases and the SPP wave becomes more and more confined to the taper until it gets localized to a nanometer spot size, dictated solely by the apex diameter, at the very end of the taper. For metals such as gold and silver, the SPP propagation length can easily reach several tens of micrometers at near-infrared wavelengths, at least if surface roughness of the taper can be reduced to sufficiently low values. Here, we chose a gold taper due to the sensitivity of silver surfaces to oxidization and the persisting technical difficulties in fabricating high-quality conical silver tapers.[39,40] Conical gold tapers are prepared by wet-chemical etching of annealed, single crystalline wires with a diameter of 125 μm (for details see Supporting Information and ref 32). As illustrated in Figure 1b, such an etching procedure results in tapers with an opening angle of 20−30° and a particularly smooth and homogeneous surface. Both, dispersionless SPP propagation over distances of tens of micrometers as well as efficient nanofocusing to spot sizes of below 20 nm, have been demonstrated for such tapers.[30,32,41] In the case of the taper depicted in Figure 1c, the scanning electron microscope (SEM) image reveals an apex radius of curvature (ROC) of 12 nm. This value is typical for our etching procedure which provides tips with ROC of down to 5 nm.[37] Such tapers show strong electric field confinement to their very apex, as illustrated in analytic field calculations presented in Figure 1d. For near-infrared (800−2000 nm), far-field illumination of the taper apex, local electric field enhancement factors of ∼9 have been measured.[42]

To replace such far-field excitation of the apex with evanescent wave excitation, we mill gratings of seven parallel slits with a width of 800 nm and a depth of 400 nm onto these tapers by focused gallium-ion beam lithography (FEI Helios 610i) at a distance of 40−50 μm from the apex. The grating period is chosen as 2.0 μm in order to facilitate grating coupling of 1.6 μm light, incident perpendicular to the taper axis, to SPP waves propagating along the taper surface. This incident wavelength is chosen for two reasons: (i) absorption and scattering losses of the SPP wave are minimized and propagation lengths of several tens of micrometers are reached[32] and (ii) the photon energy of $\hbar\omega$ = 0.77 eV is much lower than the work function of gold of η = 5.5 eV,[43] requiring a seven-photon process to lift electrons from the Fermi level to the vacuum level and induce photoelectron emission by multiphoton excitation. This high nonlinearity restricts electron emission to the sites of highest local electric field strength and thus effectively to the apex region.

For excitation, we use few-cycle light pulses at a wavelength of 1.6 μm (Figure 1e), supplied by a home-built system of noncollinear optical parametric amplifiers and difference

DOI: 10.1021/acs.nanolett.5b01513
Nano Lett. 2015, 15, 4685−4691

frequency generation (see Supporting Information and ref 44). The system supplies pulses with duration of down to two optical cycles and a pulse energy of up to 110 nJ at a repetition rate of 5 kHz. A representative interferometric autocorrelation function of the 16 fs pulses used in the present work is shown in Figure 1f. These pulses are focused inside a vacuum chamber (base pressure 5×10^{-7} mbar) to a spot diameter of 6 μm onto the grating by using an off-axis parabolic mirror with a focal length of 50.8 mm. Electron emission from the taper is spatially resolved by a microchannel plate detector (MCP, Tectra, MCP-25-D-R-P43), followed by a phosphor screen and a camera (PCO, Pixelfly USB). The MCP is placed at a distance of 15 mm from the taper apex. For PPM imaging, a silver nanowire is introduced at a short distance from the taper. Either sample or taper can be fine positioned with high precision via a three-axis piezo stage (Physik Instrumente, P-611.3S).

We now investigate photoelectron emission from these tapers. For this, we mount a taper on a nanopositioner and raster scan it through the focal plane of the laser pulses. In these experiments, the pulse energy is set to 160 pJ and electrons are detected and counted using the MCP with the detector plane mounted perpendicular to the taper axis (Figure 1a). For optical alignment, the laser power behind the taper (Figure 2a) is recorded simultaneously with the electron signal by a photodetector placed on the optical axis (Figure 2b). This shadow image allows us to determine the position of the laser focus on the taper surface with a precision given by the focal spot size of 6 μm. An image of the detected electron counts as a function of focus position is shown in Figure 2c. The contours of taper and grating are overlaid by the white dashed lines. One can see from Figure 2c that electrons are released when focusing the laser either onto the grating or onto the taper apex. For apex illumination, the electron count rate is low (<0.01 detected electrons per pulse) and the electron signal in Figure 2c is magnified by a factor of 50. Strikingly, for grating illumination a more than fifty-fold increase in electron yield to 0.6 electrons per pulse is revealed. This enhancement is seen when placing the laser focus on those grating lines closest to the apex where SPP launching is most efficient.[45] This suggests already that direct electron emission from the grating is weak because this should be homogeneous throughout the grating.

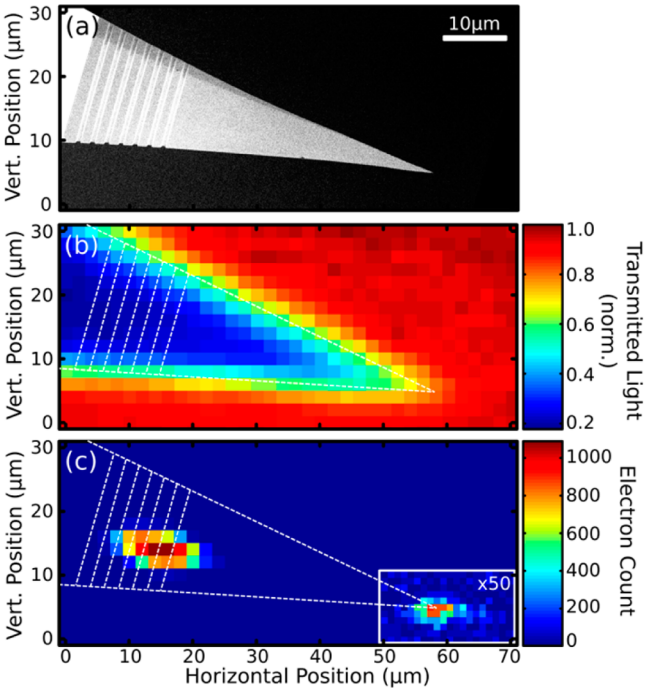

Figure 2. (a) SEM image of a gold nanotaper with grating coupler. (b) Shadow-image of the taper recorded by scanning the taper through the laser focus with a spot size of 6 μm. The laser light on the back side of the taper is measured with a photodiode. (c) Simultaneously recorded electron emission from a gold nanotaper illuminated with 160 pJ, 16 fs laser pulses centered at 1.6 μm. Electron emission is detected when placing the focus either on the grating or on the apex of the taper. The weak electron emission for apex illumination is magnified by a factor of 50. The contours of taper and grating are overlaid as white dashed lines.

Yet, we can of course not deduce direct information about the emission site of the photoelectrons from those measurements. For this, we characterize, in the next step, the spatial distribution of the electrons impinging on the MCP detector.[46] Figure 3a shows the pattern recorded when operating the taper in DC field emission mode. For this, we block the laser and apply a negative bias voltage of −250 V between tip and MCP, inducing tunnel-emission from the very apex of the taper. We observe a clean, circularly symmetric pattern, well centered on the screen. Electrons are emitted into a relatively narrow cone with an opening angle of 22°. This can be quantified by integrating the detected electron counts over the azimuthal angle φ, weighted with the area of the respective ring element to yield the radial electron distribution as a function of emission angle β with respect to the taper axis. The resulting distribution is seen as a green curve in Figure 3d and gives a $1/e$ width $\Delta\beta_{1/e}$ of 11°. Figure 3b shows the same spatial emission pattern as Figure 3a but now obtained for optical excitation of the **grating region** of the taper (pulse energy 200 pJ). Here, the DC bias voltage has been reduced to −50 V, completely suppressing DC field emission. Also, for laser-driven field emission by grating-illumination, we find a nicely symmetric, well-centered electron

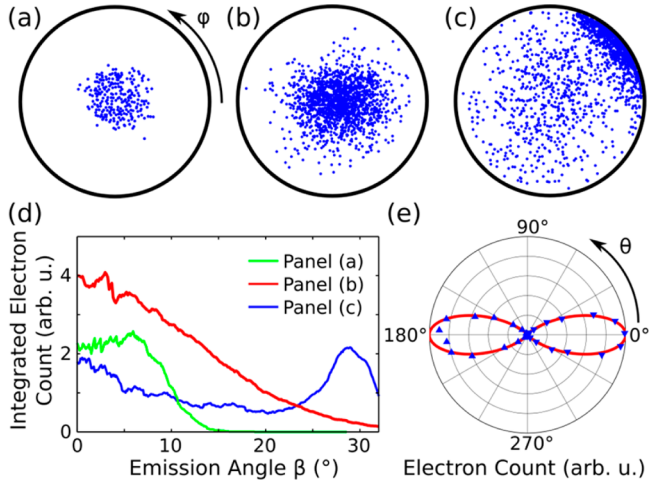

Figure 3. (a)−(c) Electron distribution on the MCP phosphor screen for emission from a sharp taper (a) by DC emission, (b) by laser illumination of the grating with low pulse energy, and (c) from a blunt taper by grating illumination with increased pulse energy. (d) Electron count integrated over the azimuthal angle φ as a function of emission angle β for the three cases. (e) Electron emission for the case of (b) as a function of the laser polarization angle θ with respect to the taper axis as a polar plot: measured values (blue symbols) and a $\cos^9\theta$ simulation (red curve).

DOI: 10.1021/acs.nanolett.5b01513
Nano Lett. 2015, 15, 4685−4691

distribution very similar to that for DC field emission. Now, the radial distribution is substantially broader (red curve in Figure 3d, $\Delta\beta_{1/e} = 18°$), most likely due to the reduced bias voltage and the less directional acceleration of the electrons in the DC near-field of the taper apex. The clear circular symmetry of both emission patterns in Figure 3a,b is taken as a strong indication that also grating illumination results in electron emission from the very apex of the taper, confirming efficient nanofocusing of the launched SPP wavepackets to the taper apex. To test this assertion, we repeat the same experiment for a blunt tip with a radius of about 50 nm. Now, the pulse energy has to be increased to 4 nJ before sizable electron emission is observed. For this tip, a completely different emission pattern emerges (Figure 3c). Now, the electrons are spread out over a much larger range of emission angles, indicating emission from a less localized source region. Most importantly, directional emission of a substantial fraction of the electrons into the upper right edge of the screen is found. The emission direction can be controlled by the relative orientation of the grating with respect to the detector plane, and hence, this is a clear signature of electron emission from the slit grating. At such high laser intensities, the field strength in the grating region is sufficient to locally induce photoemission. We find experimentally that this grating emission is only weakly dependent on the polarization direction θ of the linearly polarized incident laser. In stark contrast, we observe, for sharp tips, a quite remarkable polarization dependence. As shown in Figure 3e, the electron yield, recorded for a pulse energy of 100 pJ, shows a $\cos^9\theta$ dependence on angle, with a maximum for an incident polarization along the taper axis, maximizing coupling to SPPs. Ideally, we would have expected an even more pronounced, $\cos^{2N}\theta$ dependence due to the combined polarization sensitivity of the plasmon coupling and the Nth order nonlinearity of the multiphoton emission from the apex. We believe that this difference is mainly due to experimental limitations of our present setup. Nevertheless, we emphasize that the measured electron yield for $\theta = 90°$ is 3 orders of magnitude smaller than for zero incidence angle. Together with the symmetric and narrow angular distribution of the emission pattern (Figure 3b), this pronounced polarization dependence strongly supports that SPP launching by grating coupling results in electron emission from a single emission site at the very apex of the taper.

We now use this information to estimate relevant electric field amplitudes and thus emission regimes in our experiments. For pulse energy of 160 pJ, the peak electric field strength in the laser focus is about 0.5 V/nm. Taking a previously measured field enhancement factor of $f = 9$, we estimate, for direct apex illumination, a maximum local field amplitude of ~4.5 V/nm.[37,47] In this regime, multiphoton emission dominates with a high nonlinearity of order $N = 7$.[37] Our data indicate that the area of this emission site is the same as for SPP nanofocusing. Then, the fifty-fold enhancement of the electron yield for grating illumination, observed in Figure 2c, indicates that the local field amplitude at the apex is a factor of $50^{1/(2N)} \approx 1.32$ larger than for direct apex illumination. This illustrates two important properties of our remotely driven electron source. First, adiabatic nanofocusing enhances the local amplitude of the electric field that is incident on the grating coupler (0.5 V/nm) by approximately a factor of 12 to 6 V/nm at the very apex of the conical gold taper. The incident field amplitude of 0.5 V/nm is far too low to induce electron emission for such long wavelength laser pulses.[37] Thus, for such sharp tips, electron emission from the grating region and also from the shaft of the taper is completely negligible. Only in a nanometer-sized region at the taper apex, the enhanced field strength is sufficient to trigger photoemission, resulting in a spatially isolated and ultrafast source of photoelectrons. Moreover, our experiments also demonstrate that this electron emission is induced at exceedingly low pulse energies. Because the pulse energy scales with the product of the square of the local field amplitude and the focal area, the enhancement in field amplitude and the corresponding reduction in spot area from 30 μm^2 to ~500 nm^2 upon nanofocusing shows that approximately one out of 1000 incident photons is coupled to the taper and subsequently nanofocused to the very apex. This results in an energy of the nanofocused laser pulse of only ~250 fJ and suggests that electron emission is induced by merely 2×10^6 photons per pulse. Recently, even higher plasmon to hot electron conversion efficiencies of up to 30% have been reported in a Schottky diode configuration.[33]

To illustrate the potential and as a first application of this new electron source, we have implemented it in a point-projection microscopy setup. For this, we have dispersed single silver nanowires with a diameter of nominally 100 nm on a transmission electron microscope (TEM) grid (Figure 4a), see

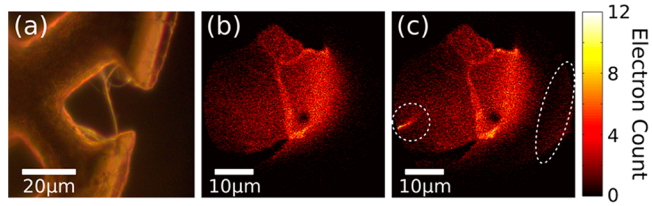

Figure 4. (a) Dark-field microscopy image of a silver nanowire deposited on a TEM grid. (b) Point projection electron microscopy image of the nanowire recorded by apex illumination of a moderately sharp taper at a laser pulse energy of 1.6 nJ. (c) Image recorded with the same pulse energy by grating illumination and remote-photoemission from the apex. Weak electron emission from the grating area is highlighted by the dashed ellipses.

Supporting Information for nanowire synthesis). This TEM grid is then mounted on a nanopositioner and placed at a distance of about 30 μm in front of the taper, as sketched in Figure 1a. To discern contributions of electrons emitted directly from the grating and remotely from the apex, we first compare PPM images recorded by direct apex illumination and grating coupling for a taper with an enlarged ROC of ~30 nm (Figure 4b,c). To obtain a sufficient number of photoelectrons from this rather blunt taper, the incident pulse energy is set to 1.6 nJ. This power level is high enough to induce weak photoemission from the grating coupler region. In both images, the structure of the nanowire is well discerned and the electron count is enhanced in the geometric shadow of the wire. Both images appear very similar and branching of the wires is resolved in the upper part of the images. For grating coupling, slight additional features appear (Figure 4c). First, there is sharp, stripe-like signal in the lower left corner (dotted circle), reflecting electron emission from the grating. Also, we find faint grating emission in the region marked by a white ellipse.

This grating-emission is completely suppressed when using grating coupling on tapers with a sharp apex. This is demonstrated in Figure 5, which shows PPM images of the same nanowire recorded with a sharp tip for three distances between tip and sample. Figure 5a is a lower magnification

DOI: 10.1021/acs.nanolett.5b01513
Nano Lett. 2015, 15, 4685−4691

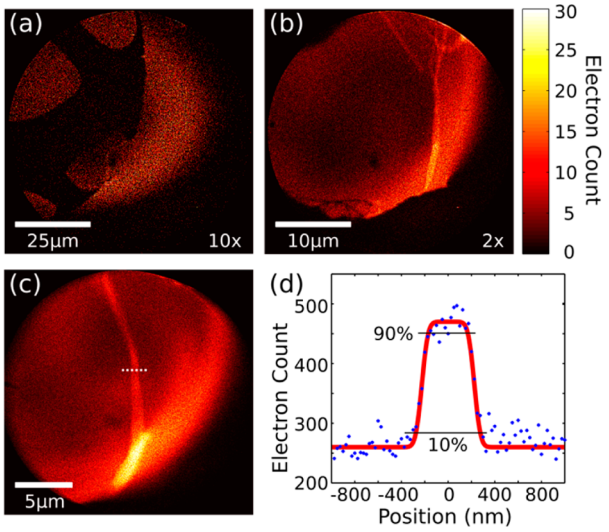

Figure 5. (a)−(c) Point projection electron microscope images from a Ag nanowire recorded by SPP nanofocusing for three decreasing taper-sample distances, that is, with increasing magnification. (d) Cross section along the white line in (c). The electron count rate is depicted by blue circles, and the red curve is a flat top profile with an edge sharpness of 110 nm.

image (M ∼ 220) recorded at a tip−sample distance of 60 μm. Here, the shape of the TEM grid appears as a dark shadow region in the image. When increasing the magnification to M ∼ 540 (tip−sample distance 24 μm), the branched nanowire is resolved and appears bright (Figure 5b). Upon a further increase in magnification (M ∼ 830 at a distance of 15 μm, Figure 5c), the edges of the wire are clearly resolved. A rectangular profile of the electron signal across the wire is observed. In the region of the wire, the electron signal increases by a factor of ∼2. The cross section in Figure 5d shows a width of ∼450 nm and an edge steepness of 110 nm. This width varies slightly along the wire. Similar rectangular cross sections have been observed in several PPM experiments before.[23,48] The inverted contrast and increased width compared to the wire diameter is readily explained by the well-known biprism effect.[49] The Ag nanowire acts as a beam splitter for the divergent electron wave and wave interference is imaged by the MCP detector. In our experiments, interference fringes are washed out due to the limited resolution of the setup and the averaged intensity is measured. The shape of the image is sensitive to weak static electric fields at the wire surface and for our low energy electrons, small potential variations of only few hundred mV are sufficient to vary both the width and the image contrast. In essence, these PPM images and specifically the sharp edges of the wire signal support our conclusion that electron emission stems only from the apex region of the taper. It is known that by grating coupling different angular momentum SPP eigenmodes of the taper are excited.[50] Out of these modes, only the lowest order, circularly symmetric (n = 0) TM0 mode propagates all the way to the apex where it is spatially confined and induces electron emission. All higher order angular momentum modes decouple from the taper already at distances of the order of one wavelength. Therefore, the overall light-to-plasmon conversion efficiency can be further enhanced by optimizing the coupling to the TM0 mode.

In order to directly measure the temporal duration of the optical field at the taper apex after adiabatic nanofocusing, we perform an interferometric autocorrelation (IAC) measurement, illuminating the conical taper with a phase-locked pair of optical pulses and detecting the electron yield as a function of the time delay between the pulse pair. Figure 6a shows the IAC

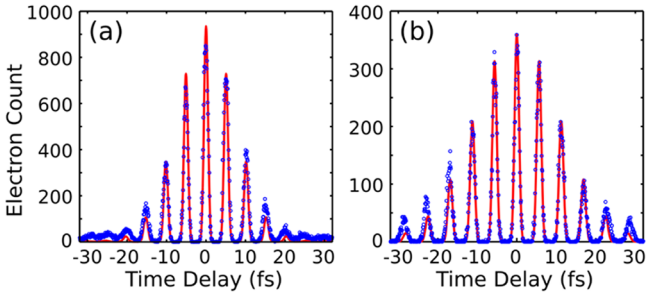

Figure 6. (a) Interferometric autocorrelation measurement (blue) and simulation (red) using the electron yield from direct apex illumination with a laser pulse pair. A laser pulse duration of 18 fs is obtained. (b) Interferometric autocorrelation measurement (blue) and simulation (red) for illumination of the grating coupler with 350 pJ pulse energy. The pulse duration of the optical field at the apex is 27 fs.

when the taper apex is illuminated directly. The measurements agree well with simulations assuming a Gaussian pulse shape with a transform limited pulse duration of 18 fs (fwhm), a central wavelength of 1530 nm and a five-photon process for electron emission. Small deviations for longer time delays are due to a small amount of residual chirp on the laser pulses. This reproduces well the pulse duration of the illuminating laser shown in Figure 1f.

Illuminating the grating coupler with a moderate pulse energy of 350 pJ to ensure electron emission solely from the taper apex, the IAC becomes slightly longer (see Figure 6b). We can simulate the IAC well by assuming again a fifth order nonlinearity and by taking a Gaussian profile of the optical field at the taper apex with a pulse duration of 27 fs (fwhm) and a central wavelength shifted to 1690 nm. The increase in pulse duration and this shift in wavelength reflect the finite bandwidth of our grating coupler. The bandwidth can be further enlarged by optimizing the grating coupler and, together with a careful dispersion management, a pulse duration of down to 10 fs can be reached.[32]

In summary, we have described and demonstrated a novel and highly compact source of ultrafast electron pulses. When launching surface plasmon polariton wavepackets on the shaft of a sharp, conical gold taper, we find that electrons are emitted from the very apex of this taper by multiphoton emission with a yield that exceeds that for direct apex illumination by a factor of more than 50. Point-projection microscopy images verify that all detected photoelectrons are indeed emitted from a nanometer-sized spot at the tip apex. This underlines the unique nanofocusing capabilities of such adiabatic tapers. An incident laser with a focal spot area of 30 μm^2 is compressed into an area of merely 500 nm^2 upon nanofocusing. The concomitant field enhancement is so strong that electrons are emitted at focused pulse energies of only few hundred femtojoules.

This intriguing source carries potential for various types of applications. First, the absence of any direct apex illumination for nanotip photoemission will allow for particularly compact point-projection microscopy setups with micrometer-sized emitter−sample distance. This will allow for preserving the intrinsically short, few-femtosecond duration of the ejected electron pulses and, thus, enable point projection electron

DOI: 10.1021/acs.nanolett.5b01513
Nano Lett. 2015, 15, 4685−4691

microscopy and holography with unprecedented time resolution. Second, the mesoscopic spatial separation between optical excitation and electron emission site is crucially beneficial for integrating such tapers into ultracompact electron gun designs and thus for tailoring electron beams with femtosecond pulse duration. In particular, when combining our electron source with high-repetition rate few-cycle near-infrared fiber lasers,[51] we expect single electron generation with sufficient brightness for a variety of applications in ultrafast electron microscopy and diffraction. Also, it is obvious that the high demonstrated electric field strength at the apex will not only trigger photoelectron emission but also high order optical nonlinearities. It will be interesting to study high optical harmonic generation from this point-like light source. Finally, the exceedingly low pulse energy of the focused plasmon pulses effectively reduces taper heating and thermal expansion and, thus, has the potential to overcome one of the most challenging problems in current implementations of ultrafast scanning tunneling microscopy.

■ ASSOCIATED CONTENT

Supporting Information

Fabrication of single-crystalline gold tapers, details on the pulsed laser light source and the experimental setup, synthesis of Ag nanowires. The Supporting Information is available free of charge on the ACS Publications website at DOI: 10.1021/acs.nanolett.5b01513.

■ AUTHOR INFORMATION

Corresponding Authors

*E-mail: petra.gross@uni-oldenburg.de.
*E-mail: christoph.lienau@uni-oldenburg.de.

Notes

The authors declare no competing financial interest.

■ ACKNOWLEDGMENTS

The authors thank Benedikt Nickel for support with the image recording hard- and software. Financial support by the Deutsche Forschungsgemeinschaft (SPP1391, SPP1839, and DFG-NSF Materials World Network), by the European Union (project "CRONOS", grant number 280879-2) and the Korea Foundation for International Cooperation of Science and Technology (Global Research Laboratory project, K20815000003) is gratefully acknowledged. J.V., J.R., B.N., P.D., and D.R. acknowledge personal grants from the Studienstiftung des Deutschen Volkes, the Deutsche Forschungsgemeinschaft (Research Training Group "Molecular Basis of Sensory Biology"), the German Academic Exchange Service (IPID4all program), the Campus Hungary program, the Hungarian Academy of Sciences ("Lendület" grant) and the Stiftung der Metallindustrie im Nord-Westen.

■ REFERENCES

(1) Batson, P. E.; Dellby, N.; Krivanek, O. L. *Nature* **2002**, *418*, 617−620.
(2) Mourou, G.; Williamson, S. *Appl. Phys. Lett.* **1982**, *41*, 44−45.
(3) Williamson, S.; Mourou, G.; Li, J. C. M. *Phys. Rev. Lett.* **1984**, *52*, 2364−2367.
(4) Aeschlimann, M.; Hull, E.; Cao, J.; Schmuttenmaer, C. A.; Jahn, L. G.; Gao, Y.; Elsayedali, H. E.; Mantell, D. A.; Scheinfein, M. R. *Rev. Sci. Instrum.* **1995**, *66*, 1000−1009.
(5) Williamson, J. C.; Zewail, A. H. *Proc. Natl. Acad. Sci. U.S.A.* **1991**, *88*, 5021−5025.
(6) Zewail, A. H. *Science* **2010**, *328*, 187−193.
(7) Siwick, B. J.; Dwyer, J. R.; Jordan, R. E.; Miller, R. J. D. *Science* **2003**, *302*, 1382−1385.
(8) Mankowsky, R.; Subedi, A.; Foerst, M.; Mariager, S. O.; Chollet, M.; Lemke, H. T.; Robinson, J. S.; Glownia, J. M.; Minitti, M. P.; Frano, A.; Fechner, M.; Spaldin, N. A.; Loew, T.; Keimer, B.; Georges, A.; Cavalleri, A. *Nature* **2014**, *516*, 71−73.
(9) Grupp, A.; Mayer, B.; Schmidt, C.; Oelmann, J.; Marvel, R. E.; Haglund, R. F.; Leitenstorfer, A.; Pashkin, A. *Ultrafast Phenomena XIX*; Springer: New York, 2015.
(10) Pashkin, A.; Kuebler, C.; Ehrke, H.; Lopez, R.; Halabica, A.; Haglund, R. F., Jr.; Huber, R.; Leitenstorfer, A. *Phys. Rev. B* **2011**, *83*, 195120.
(11) Falke, S. M.; Rozzi, C. A.; Brida, D.; Maiuri, M.; Amato, M.; Sommer, E.; De Sio, A.; Rubio, A.; Cerullo, G.; Molinari, E.; Lienau, C. *Science* **2014**, *344*, 1001−1005.
(12) Kassier, G. H.; Haupt, K.; Erasmus, N.; Rohwer, E. G.; Schwoerer, H. *J. Appl. Phys.* **2009**, *105*, 113111.
(13) Fill, E.; Veisz, L.; Apolonski, A.; Krausz, F. *New J. Phys.* **2006**, *8*, 272.
(14) van Oudheusden, T.; Pasmans, P.; van der Geer, S.; de Loos, M.; van der Wiel, M.; Luiten, O. *Phys. Rev. Lett.* **2010**, *105*, 264801.
(15) Gao, M.; Lu, C.; Jean-Ruel, H.; Liu, L. C.; Marx, A.; Onda, K.; Koshihara, S.-y.; Nakano, Y.; Shao, X.; Hiramatsu, T.; Saito, G.; Yamochi, H.; Cooney, R. R.; Moriena, G.; Sciaini, G.; Miller, R. J. D. *Nature* **2013**, *496*, 343−346.
(16) Wimmer, L.; Herink, G.; Solli, D. R.; Yalunin, S. V.; Echternkamp, K. E.; Ropers, C. *Nat. Phys.* **2014**, *10*, 432−436.
(17) Veisz, L.; Kurkin, G.; Chernov, K.; Tarnetsky, V.; Apolonski, A.; Krausz, F.; Fill, E. *New J. Phys.* **2007**, *9*, 451.
(18) Fink, H. W.; Stocker, W.; Schmid, H. *Phys. Rev. Lett.* **1990**, *65*, 1204−1206.
(19) Beyer, A.; Goelzhaeuser, A. *J. Phys.: Condens. Matter* **2010**, *22*, 343001.
(20) Longchamp, J.-N.; Escher, C.; Latychevskaia, T.; Fink, H.-W. *Ultramicroscopy* **2014**, *145*, 80−84.
(21) Quinonez, E.; Handali, J.; Barwick, B. *Rev. Sci. Instrum.* **2013**, *84*, 103710.
(22) Ehberger, D.; Hammer, J.; Eisele, M.; Krueger, M.; Noe, J.; Hoegele, A.; Hommelhoff, P. Highly coherent electron beam from a laser-triggered tungsten needle tip. 2014, *arXiv:1412.4584*. arXiv.org e-Print archive. http://arxiv.org/abs/1412.4584 (accessed May 2014).
(23) Müller, M.; Paarmann, A.; Ernstorfer, R. *Nature Commun.* **2014**, *5*, 5292.
(24) Ropers, C.; Solli, D. R.; Schulz, C. P.; Lienau, C.; Elsaesser, T. *Phys. Rev. Lett.* **2007**, *98*, 043907.
(25) Hommelhoff, P.; Sortais, Y.; Aghajani-Talesh, A.; Kasevich, M. A. *Phys. Rev. Lett.* **2006**, *96*, 077401.
(26) Babadjanyan, A. J.; Margaryan, N. L.; Nerkararyan, K. V. *J. Appl. Phys.* **2000**, *87*, 3785−3788.
(27) Stockman, M. I. *Phys. Rev. Lett.* **2004**, *93*, 137404.
(28) Gramotnev, D. K.; Bozhevolnyi, S. I. *Nat. Photonics* **2010**, *4*, 83−91.
(29) Ropers, C.; Neacsu, C. C.; Elsaesser, T.; Albrecht, M.; Raschke, M. B.; Lienau, C. *Nano Lett.* **2007**, *7*, 2784−2788.
(30) Neacsu, C. C.; Berweger, S.; Olmon, R. L.; Saraf, L. V.; Ropers, C.; Raschke, M. B. *Nano Lett.* **2010**, *10*, 592−596.
(31) Berweger, S.; Atkin, J. M.; Xu, X. G.; Olrnon, R. L.; Raschke, M. B. *Nano Lett.* **2011**, *11*, 4309−4313.
(32) Schmidt, S.; Piglosiewicz, B.; Sadiq, D.; Shirdel, J.; Lee, J. S.; Vasa, P.; Park, N.; Kim, D.-S.; Lienau, C. *ACS Nano* **2012**, *6*, 6040−6048.
(33) Giugni, A.; Torre, B.; Toma, A.; Francardi, M.; Malerba, M.; Alabastri, A.; Proietti Zaccaria, R.; Stockman, M. I.; Di Fabrizio, E. *Nat. Nanotechnol.* **2013**, *8*, 845−852.
(34) Keathley, P. D.; Sell, A.; Putnam, W. P.; Guerrera, S.; Velasquez-Garcia, L.; Kartner, F. X. *Ann. Phys. (Berlin, Ger.)* **2013**, *525*, 144−150.
(35) Krüger, M.; Schenk, M.; Hommelhoff, P. *Nature* **2011**, *475*, 78−81.

DOI: 10.1021/acs.nanolett.5b01513
Nano Lett. 2015, 15, 4685−4691

(36) Herink, G.; Solli, D. R.; Gulde, M.; Ropers, C. *Nature* **2012**, *483*, 190−193.
(37) Piglosiewicz, B.; Schmidt, S.; Park, D. J.; Vogelsang, J.; Grosz, P.; Manzoni, C.; Farinello, P.; Cerullo, G.; Lienau, C. *Nat. Photon* **2014**, *8*, 37−42.
(38) Gulde, M.; Schweda, S.; Storeck, G.; Maiti, M.; Yu, H. K.; Wodtke, A. M.; Schaefer, S.; Ropers, C. *Science* **2014**, *345*, 200−204.
(39) Kalbacova, J.; Rodriguez, R. D.; Desale, V.; Schneider, M.; Amin, I.; Jordan, R.; Zahn, D. R. T. *Nanospectroscopy* **2015**, *1*, 12−18.
(40) Sasaki, S. S.; Perdue, S. M.; Perez, A. R.; Tallarida, N.; Majors, J. H.; Apkarian, V. A.; Lee, J. *Rev. Sci. Instrum.* **2013**, *84*, 096109.
(41) Sadiq, D.; Shirdel, J.; Lee, J. S.; Selishcheva, E.; Park, N.; Lienau, C. *Nano Lett.* **2011**, *11*, 1609−1613.
(42) Park, D. J.; Piglosiewicz, B.; Schmidt, S.; Kollmann, H.; Mascheck, M.; Lienau, C. *Phys. Rev. Lett.* **2012**, *109*, 244803.
(43) Sachtler, W. M.; Dorgelo, G. J. H.; Holscher, A. A. *Surf. Sci.* **1966**, *5*, 221−229.
(44) Vogelsang, J.; Robin, J.; Piglosiewicz, B.; Manzoni, C.; Farinello, P.; Melzer, S.; Feru, P.; Cerullo, G.; Lienau, C.; Gross, P. *Opt. Express* **2014**, *22*, 25295−306.
(45) Kim, D. S.; Hohng, S. C.; Malyarchuk, V.; Yoon, Y. C.; Ahn, Y. H.; Yee, K. J.; Park, J. W.; Kim, J.; Park, Q. H.; Lienau, C. *Phys. Rev. Lett.* **2003**, *91*, 143901.
(46) Bormann, R.; Gulde, M.; Weismann, A.; Yalunin, S. V.; Ropers, C. *Phys. Rev. Lett.* **2010**, *105*, 147601.
(47) Park, D. J.; Piglosiewicz, B.; Schmidt, S.; Kollmann, H.; Mascheck, M.; Gross, P.; Lienau, C. *Ann. Phys. (Berlin, Ger.)* **2013**, *525*, 135−142.
(48) Lai, W.; Degiovanni, A.; Morin, R. *Appl. Phys. Lett.* **1999**, *74*, 618−620.
(49) Möllenstedt, G.; Düker, H. *Z. Phys.* **1956**, *145*, 377−397.
(50) Esmann, M.; Becker, S. F.; da Cunha, B. B.; Brauer, J. H.; Vogelgesang, R.; Gross, P.; Lienau, C. *Beilstein J. Nanotechnol.* **2013**, *4*, 603−610.
(51) Krauss, G.; Lohss, S.; Hanke, T.; Sell, A.; Eggert, S.; Huber, R.; Leitenstorfer, A. *Nat. Photonics* **2010**, *4*, 33−36.

DOI: 10.1021/acs.nanolett.5b01513
Nano Lett. 2015, 15, 4685−4691